Journal of Computational Mathematics, Vol.27, No.2-3, 2009, 338–347.

A NOTE ON PRESSURE APPROXIMATION OF FIRST AND HIGHER ORDER PROJECTION SCHEMES FOR THE NONSTATIONARY INCOMPRESSIBLE NAVIER-STOKES EQUATIONS*

Erich Carelli and Andreas Prohl
Mathematisches Institut, Universität Tübingen, Auf der Morgenstelle 10, D-72076 Tübingen
Email: carelli@na.uni-tuebingen.de, prohl@na.uni-tuebingen.de

Abstract

Projection methods are efficient operator-splitting schemes to approximate solutions of the incompressible Navier-Stokes equations. As a major drawback, they introduce spurious layers, both in space and time. In this work, we survey convergence results for higher order projection methods, in the presence of only strong solutions of the limiting problem; in particular, we highlight concomitant difficulties in the construction process of accurate higher order schemes, such as limited regularities of the limiting solution, and a lack of accurate initial data for the pressure. Computational experiments are included to compare the presented schemes, and illustrate the difficulties mentioned.

Mathematics subject classification: 65N22, 65F05, 65M15, 35K55, 35Q30.
Key words: Incompressible Navier-Stokes equation, Time discretization, Projection method.

1. Introduction

Let $\Omega \subset \mathbb{R}^d$, for $d = 2, 3$ be a bounded Lipschitz domain, and $T > 0$; we consider the time-dependent Navier-Stokes equations for incompressible, viscous ($\nu > 0$) Newtonian fluids,

$$\mathbf{u}_t - \nu\Delta\mathbf{u} + (\mathbf{u}\cdot\nabla)\mathbf{u} + \nabla p = \mathbf{f} \quad \text{in } \Omega_T := (0,T)\times\Omega, \tag{1.1}$$

$$\operatorname{div}\mathbf{u} = 0 \qquad \text{in } \Omega_T, \tag{1.2}$$

$$\mathbf{u} = \mathbf{0} \qquad \text{on } \partial\Omega_T := (0,T)\times\partial\Omega, \tag{1.3}$$

$$\mathbf{u}(0,\cdot) = \mathbf{u}_0 \quad \text{in } \Omega. \tag{1.4}$$

Here, $\mathbf{u} : \Omega_T \to \mathbb{R}^d$ denotes the velocity field, $p : \Omega_T \to \mathbb{R}$ the scalar pressure of vanishing mean value, i.e., $\int_\Omega p(\cdot,\mathbf{x})\,\mathrm{d}\mathbf{x} = 0$, and a given force $\mathbf{f} : \Omega_T \to \mathbb{R}^d$ is driving the fluid flow, with initial velocity field $\mathbf{u}_0 : \Omega \to \mathbb{R}^d$.

In the following, we approximate strong solutions $\mathbf{u} \in W^{1,2}\big(0,T;\mathbf{J}_0(\Omega)\big) \cap L^2\big(0,T;\mathbf{J}_1(\Omega) \cap \mathbf{W}^{2,2}(\Omega)\big)$ of (1.1)-(1.4), whose existence for data

$$\mathbf{u}_0 \in \mathbf{J}_1(\Omega), \quad \mathbf{f} \in L^2\big(0,T;\mathbf{J}_0(\Omega)\big)$$

is well-known to be (at least) local ($d = 3$) resp. global ($d = 2$). Here and below, we adopt the standard notation of Sobolev and Bochner spaces, and use the notation

$$\mathbf{J}_0(\Omega) = \big\{\mathbf{v} \in \mathbf{L}^2(\Omega) : \operatorname{div}\mathbf{v} = 0 \ \text{ weakly in } \Omega,\ \langle\mathbf{v},\mathbf{n}\rangle = 0 \text{ on } \partial\Omega\big\},$$
$$\mathbf{J}_1(\Omega) = \big\{\mathbf{v} \in \mathbf{W}_0^{1,2}(\Omega) : \operatorname{div}\mathbf{v} = 0 \ \text{ weakly in } \Omega\big\},$$

* Received December 12, 2007 / Revised version received June 12, 2008 / Accepted July 14, 2008 /

where $\langle\cdot,\cdot\rangle$ denotes the standard scalar product in $\mathbb{R}^d$, and $\mathbf{n}(\mathbf{x}) \in \mathbb{S}^{d-1}$ is the unit vector field pointing outside Ω.

Recall that solutions of (1.1)-(1.4) suffer a breakdown of regularity for $t \to 0$, even in the case of smooth (initial) data. Global regularity would require data $\mathbf{u}_0$ and $\mathbf{f}$ to satisfy a nonlocal compatibility condition which is virtually uncheckable in actual cases: it is proved in [5] that global regularity may only be valid if there exists a solution $p_0 \in W^{1,2}(\Omega) \cap L^2_0(\Omega)$ of the overdetermined Neumann problem

$$\begin{aligned} \Delta p_0 &= \operatorname{div}\big(\mathbf{f}(0,\cdot) - (\mathbf{u}_0 \cdot \nabla)\mathbf{u}_0\big) \qquad \text{in } \Omega, \\ \nabla p_0 &= \nu \Delta \mathbf{u}_0 + \mathbf{f}(0,\cdot) - (\mathbf{u}_0 \cdot \nabla)\mathbf{u}_0 \quad \text{on } \partial\Omega. \end{aligned}$$

In order to justify existence of (local) strong solutions, we always suppose that the data in (1.1)-(1.4) satisfy

(A1) (regularity of domain) The unique solution $\mathbf{w} \in \mathbf{J}_1(\Omega)$ of the stationary, incompressible Stokes problem

$$-\nu\Delta\mathbf{w} + \nabla\pi = \mathbf{g} \quad \text{in } \Omega \subset \mathbb{R}^d$$

is already in $\mathbf{J}_1(\Omega) \cap \mathbf{W}^{2,2}(\Omega)$, provided $\mathbf{g} \in \mathbf{L}^2(\Omega)$, and satisfies

$$\|\mathbf{w}\|_{\mathbf{W}^{2,2}} \le C \, \|\mathbf{g}\|_{\mathbf{L}^2}.$$

(A2) (regularity of data) For any $T > 0$, let

$$\mathbf{u}_0 \in \mathbf{J}_1(\Omega) \cap \mathbf{W}^{2,2}(\Omega),$$

$$\mathbf{f} \in W^{2,\infty}\big(0,T;\mathbf{L}^2(\Omega)\big).$$

A second-order temporal discretization of (1.1)-(1.4) uses the Crank-Nicholson method; in [6], it has been shown that iterates $\{(\mathbf{u}^m, p^m)\}_{m>0}$ satisfy

$$\max_{1\le m\le M} \tau_m \Big[\|\mathbf{u}(t_m,\cdot) - \mathbf{u}^m\|_{\mathbf{L}^2} + \sqrt{\tau_m} k \, \|p(t_m,\cdot) - p^{m-1/2}\|_{L^2} \Big] \le Ck^2, \tag{1.5}$$

where

$$\tau_m := \min\{1, t_m\}, \quad p^{m-1/2} = \frac{1}{2}\{p^m + p^{m-1}\}.$$

The practical disadvantage of implicit discretization strategies of (1.1)-(1.4) is the significant computational effort implied from the necessity to solve coupled nonlinear algebraic problems to determine (Galerkin approximations of) $(\mathbf{u}^m, p^m)$ at every time-step given by $1 \le m \le M$. As a consequence, splitting algorithms were developed to reduce complexity of actual computations; among them, and one of the first, is Chorin's projection method [1, 2, 13], where iterates for velocity field and pressure are independently obtained at every time-step. However, it is known that the quality of pressure iterates is deteriorated by unphysical boundary layers [3, 10]. One strategy to improve their quality is to either construct (formally) first-order schemes which are exempted from this deficiency (i.e., the Chorin-Uzawa scheme [7, Section 8], or Chorin-Penalty scheme [9]), whereas another one would be to construct higher order projection schemes, where possible boundary layers are less pronounced (i.e., the Van Kan scheme [14]). The Van Kan

scheme formally combines the ideas of second-order time discretization (Crank-Nicholson) and projection. For its formulation, we use notations $d_t\phi^m := k^{-1}\{\phi^m - \phi^{m-1}\}$, where $k = t_m - t_{m-1} > 0$ is the (equi-distant) time-step, and $\phi^{m-1/2} := \frac{1}{2}\{\phi^m + \phi^{m-1}\}$. Moreover, we denote $\mathbf{f}^m := \mathbf{f}(t_m, \cdot)$. Then, the scheme reads:

Algorithm 1.1. *1. Let $m \geq 1$, and $\big(\mathbf{u}^{m-1}, \tilde{\mathbf{u}}^{m-1}, p^{m-1}\big) \in \mathbf{J}_0(\Omega) \times \mathbf{W}_0^{1,2}(\Omega) \times L_0^2(\Omega)$ be given. Find $\tilde{\mathbf{u}}^m \in \mathbf{W}_0^{1,2}(\Omega)$ such that*

$$\frac{1}{k}\{\tilde{\mathbf{u}}^m - \mathbf{u}^{m-1}\} - \nu\Delta\tilde{\mathbf{u}}^{m-1/2} + \frac{1}{2}(\mathbf{P}_{\mathbf{J}_0}\tilde{\mathbf{u}}^m \cdot \nabla)\tilde{\mathbf{u}}^m + \frac{1}{2}(\mathbf{u}^{m-1} \cdot \nabla)\tilde{\mathbf{u}}^{m-1} + \nabla p^{m-1} = \mathbf{f}^{m-1/2} \quad \text{in } \Omega. \tag{1.6}$$

2. Given $\big(\tilde{\mathbf{u}}^m, p^{m-1}\big) \in \mathbf{W}_0^{1,2}(\Omega) \times L_0^2(\Omega)$, find $\big(\mathbf{u}^m, p^m\big) \in \mathbf{J}_0(\Omega) \times \big[L_0^2(\Omega) \cap W^{1,2}(\Omega)\big]$ from

$$\frac{1}{k}\{\mathbf{u}^m - \tilde{\mathbf{u}}^m\} + \frac{1}{2}\nabla[p^m - p^{m-1}] = \mathbf{0}, \quad \operatorname{div}\mathbf{u}^m = 0 \quad \text{in } \Omega, \tag{1.7}$$

$$\langle \mathbf{u}^m, \mathbf{n}\rangle = 0 \quad \text{on } \partial\Omega. \tag{1.8}$$

In (1.6), we choose an implicit discretization for the convection term, with orthogonal projection $\mathbf{P}_{\mathbf{J}_0} : \mathbf{L}^2(\Omega) \to \mathbf{J}_0(\Omega)$. Another admissible strategy is to replace the term $\frac{1}{2}\big(\mathbf{P}_{\mathbf{J}_0}\tilde{\mathbf{u}}^m \cdot \nabla\big)\tilde{\mathbf{u}}^m$ by $\frac{1}{2}\big[(\tilde{\mathbf{u}}^m \cdot \nabla)\tilde{\mathbf{u}}^m + \frac{1}{2}(\operatorname{div}\tilde{\mathbf{u}}^m)\tilde{\mathbf{u}}^m\big]$.

The second step can be reformulated as a problem for pressure increments,

$$-\Delta[p^m - p^{m-1}] = -\frac{1}{k}\operatorname{div}\tilde{\mathbf{u}}^m \quad \text{in } \Omega, \tag{1.9a}$$

$$\partial_{\mathbf{n}} p^{m+1} = 0 \quad \text{on } \partial\Omega, \tag{1.9b}$$

which is followed by the update $\mathbf{u}^m = \tilde{\mathbf{u}}^m - \frac{k}{2}\nabla[p^m - p^{m-1}]$.

A convergence analysis for (1.6)-(1.8) started with [11], where second-order convergence for iterates of the velocity field $\{\mathbf{u}^m\}_{m=1}^M$ in the norm $\ell^2\big(0, t_M; \mathbf{L}^2\big)$ is proved, provided the solution of (1.1) is sufficiently smooth. In [7, Section 7], (almost) optimal estimates for the velocity field are shown in $\ell^\infty\big(0, t_M; \mathbf{L}^2\big)$, while (almost) first-order is verified for pressure iterates in $\ell^2\big(0, t_M; L_0^2\big)$, i.e.,

$$\max_{1\leq m\leq M} \sqrt{\tau_m}\Big[\|\mathbf{u}(t_m, \cdot) - \tilde{\mathbf{u}}^m\|_{\mathbf{L}^2} + k\,\|p(t_m, \cdot) - p^{m-1/2}\|_{L^2}\Big] \leq Ck^2\,|\log k|. \tag{1.10}$$

For this purpose, the proof is based on interpreting Algorithm A as a semi-explicit pressure correction scheme, with $\epsilon = \frac{1}{2}k^2$, where

$$\operatorname{div}\tilde{\mathbf{u}}^m - \epsilon\Delta d_t p^m = 0 \quad \text{in } \Omega, \tag{1.11a}$$

$$\partial_{\mathbf{n}}[p^m - p^{m-1}] = 0 \qquad \text{on } \partial\Omega, \tag{1.11b}$$

and $p^0 = p(0, \cdot)$ in Ω. Again, besides the requirement of *accurate initial data* for the pressure which is hard to validate in practice, an assumption concerning *higher regularity of solutions* for (1.1)-(1.4) is made which conflicts with the general breakdown of regularity for $t \to 0$. In order to overcome this problem and construct a stable second-order revised Van Kan scheme, certain time-mesh geometries are introduced in [7, Chapter 10], which refine at the origin $t = 0$, and

thus allow to distinguish between local mesh size $\big(k_m = (m+1)k_0^2\big)$ for temporal discretization effects, and the reference mesh size $k_0 > 0$ at times $t = \mathcal{O}(1)$ which scales the perturbation of the incompressibility constraint. Such strategies

1. are of the same asymptotic effort like equi-distant step sizes $k_0 > 0$,
2. reliably overcome the time layer at the origin $t = 0$ in the sense that the above convergence result for Algorithm A now holds for (general) strong solutions of (1.1)-(1.4), and
3. does not require accurate initial data for the pressure, and $p^0 = 0$ is sufficient.

To be precise, we introduce the mesh $\mathcal{G}_2(k_m) = \{k_m\}_{m\geq 1}$, with $t_m = \sum_{\ell=1}^m k_\ell$, and

$$k : m \mapsto k_m = \begin{cases} mk_0^2, & 0 < t_m \leq 1, \\ \gamma k_0, & t_m > 1. \end{cases} \tag{1.12}$$

Here, let $k_0 > 0$ be the basic grid size, and $\gamma = \mathcal{O}(1)$. A simple calculation shows that $t = 1$ is reached after $\sqrt{2}/k_0$ steps.

The revised Van Kan scheme in [7, Chapter 10] uses $\mathcal{G}_2(k_m)$, and $p^0 = 0$, and is stated next.

Algorithm 1.2. *1. Let $m \geq 1$, and $\big(\mathbf{u}^{m-1}, \tilde{\mathbf{u}}^{m-1}, p^{m-1}\big) \in \mathbf{J}_0(\Omega) \times \mathbf{W}_0^{1,2}(\Omega) \times L_0^2(\Omega)$ be given. Find $\tilde{\mathbf{u}}^m \in \mathbf{W}_0^{1,2}(\Omega)$ such that*

$$\begin{aligned} &\frac{1}{k_m}\big\{\tilde{\mathbf{u}}^m - \mathbf{u}^{m-1}\big\} - \nu\Delta\tilde{\mathbf{u}}^{m-1/2} + \frac{1}{2}(\mathbf{P}_{\mathbf{J}_0}\tilde{\mathbf{u}}^m \cdot \nabla)\tilde{\mathbf{u}}^m \\ &\quad + \frac{1}{2}(\mathbf{u}^{m-1} \cdot \nabla)\tilde{\mathbf{u}}^{m-1} + \frac{m-1}{m}\nabla p^{m-1} = \mathbf{f}^{m-1/2} \quad \text{in } \Omega. \end{aligned} \tag{1.13}$$

2. Given $\big(\tilde{\mathbf{u}}^m, p^{m-1}\big) \in \mathbf{W}_0^{1,2}(\Omega) \times L_0^2(\Omega)$, find $\big(\mathbf{u}^m, p^m\big) \in \mathbf{J}_0(\Omega) \times \big[L_0^2(\Omega) \cap W^{1,2}(\Omega)\big]$ from

$$\frac{1}{k_{m+1}}\big\{\mathbf{u}^m - \tilde{\mathbf{u}}^m\big\} + \frac{1}{2}\nabla\left[\frac{m}{m+1}p^m - \frac{m-1}{m+1}p^{m-1}\right] = 0, \operatorname{div}\mathbf{u}^m = 0 \quad \text{in } \Omega, \tag{1.14}$$

$$\langle \mathbf{u}^m, \mathbf{n}\rangle = 0 \quad \text{on } \partial\Omega. \tag{1.15}$$

Let us motivate the relevant effects in this algorithm; for this purpose, we distinguish between $d_t\varphi^m := \frac{1}{k_m}\big\{\varphi^m - \varphi^{m-1}\big\}$, and $\tilde{d}_t\varphi^m := \frac{1}{k_0}\big\{\varphi^m - \varphi^{m-1}\big\}$. Then $\{\tilde{\mathbf{u}}^m\}_{m>0} \subset \mathbf{W}_0^{1,2}(\Omega)$ solves

$$d_t\tilde{\mathbf{u}}^m - \Delta\tilde{\mathbf{u}}^{m-1/2} + \frac{1}{2}\nabla\left[3\frac{m-1}{m}p^{m-1} - \frac{m-2}{m}p^{m-2}\right] = \mathbf{f}^{m-1/2} \quad \text{in } \Omega, \tag{1.16}$$

$$\operatorname{div}\tilde{\mathbf{u}}^m - \frac{1}{2}k_0^2\tilde{d}_t\mathcal{P}^m = 0 \quad \text{in } \Omega, \tag{1.17}$$

$$\partial_{\mathbf{n}}\tilde{d}_t\mathcal{P}^m = 0 \quad \text{in } \partial\Omega, \quad p^m = \frac{1}{mk_0}\mathcal{P}^m. \tag{1.18}$$

Hence, we observe a decoupling of scales reflecting time discretization, and perturbation of the incompressibility constraint. In fact, one motivation to use the mesh $\mathcal{G}_2(k_m)$ at this place is

optimal convergence behavior of solutions $\big(\mathbf{u}^\epsilon, p^\epsilon\big) : \Omega_T \to \mathbb{R}^d \times \mathbb{R}$ for $\epsilon \to 0$ of $\big(\tau := \min\{1, t\}$, and $r \geq 2\big)$

$$\begin{aligned}
&\mathbf{u}_t^\epsilon - \nu\Delta\mathbf{u}^\epsilon + \big(\mathbf{P}_{\mathbf{J}_0}\mathbf{u}^\epsilon \cdot \nabla\big)\mathbf{u}^\epsilon + \nabla p^\epsilon = \mathbf{f} \quad \text{in } \Omega_T,\\
&\operatorname{div}\mathbf{u}^\epsilon - \epsilon\Delta\big\{\tau^r p^\epsilon\big\}_t = 0 \quad \text{in } \Omega_T,\\
&\partial_{\mathbf{n}}\big\{\tau^r p^\epsilon\big\}_t = 0 \qquad\qquad \text{in } \partial\Omega_T,
\end{aligned}$$

towards (general) strong solutions of (1.1)-(1.4); cf. [9, Chapter 4]. — The following convergence behavior for iterates $\big\{\big(\tilde{\mathbf{u}}^m, p^m\big)\big\}_{m>0}$ of Algorithm B has been verified in [7, Chapter 10].

$$\begin{aligned}
&\max\Big[\|\mathbf{u}(t_m,\cdot) - \mathbf{u}^{m-1/2}\|_{\mathbf{L}^2} + k_0\,\|p(t_m,\cdot) - p^{m-1/2}\|_{L^2}\Big]\\
&\leq Ck_0^2\Big[1 + |\log k_0|\Big]. \qquad (1.19)
\end{aligned}$$

A different strategy to improve the accuracy of pressure iterates from e.g. Chorin's scheme is realized in the following first-order projection scheme, where well-known artificial boundary layers in the pressure in Chorin's scheme [1,2,13] are removed. In the following, let $\tilde{p}^0 = p^0 = 0$, and $\beta \geq 1$.

Algorithm 1.3. *1. For $1 \leq m \leq M$, let $\big(\mathbf{u}^{m-1}, \tilde{\mathbf{u}}^{m-1}, p^{m-1}, \tilde{p}^{m-1}\big) \in \mathbf{J}_0(\Omega) \times \mathbf{W}_0^{1,2}(\Omega) \times \big[L_0^2(\Omega)\big]^2$ be given. Find $\tilde{\mathbf{u}}^m \in \mathbf{W}_0^{1,2}(\Omega)$ such that*

$$\begin{aligned}
&\frac{1}{k}\big\{\tilde{\mathbf{u}}^m - \mathbf{u}^{m-1}\big\} - \beta\,\nabla\operatorname{div} d_t\tilde{\mathbf{u}}^m - \nu\Delta\tilde{\mathbf{u}}^m\\
&\quad + (\mathbf{u}^{m-1}\cdot\nabla)\tilde{\mathbf{u}}^m + \nabla\big\{p^{m-1} - \tilde{p}^{m-1}\big\} = \mathbf{f}^m \quad \textit{in } \Omega. \qquad (1.20)
\end{aligned}$$

2. Find $\big(\mathbf{u}^m, \tilde{p}^m\big) \in \mathbf{J}_0(\Omega) \times L_0^2(\Omega)$ that solves

$$\begin{aligned}
&\frac{1}{k}\big\{\mathbf{u}^m - \tilde{\mathbf{u}}^m\big\} + \nabla\tilde{p}^m = 0, \quad \operatorname{div}\mathbf{u}^m = 0 \quad \textit{in } \Omega, \qquad (1.21)\\
&\langle\mathbf{u}^m, \mathbf{n}\rangle = 0 \quad \textit{on } \partial\Omega\,. \qquad (1.22)
\end{aligned}$$

3. Determine $p^m \in L_0^2(\Omega)$ from

$$p^m = -\frac{1}{k}\operatorname{div}\tilde{\mathbf{u}}^m \quad \textit{in } \Omega. \qquad (1.23)$$

By eliminating $\tilde{p}^m$ from the scheme, we obtain the following reformulation of Algorithm C as a semi-explicit penalty method [7, 9],

$$\begin{aligned}
&d_t\tilde{\mathbf{u}}^m - \beta\,\nabla\operatorname{div} d_t\tilde{\mathbf{u}}^m - \nu\Delta\tilde{\mathbf{u}}^m + (\mathbf{u}^{m-1}\cdot\nabla)\tilde{\mathbf{u}}^m + \nabla p^{m-1} = \mathbf{f}^m \quad \text{in } \Omega, \qquad (1.24)\\
&\operatorname{div}\tilde{\mathbf{u}}^m + k\,p^m = 0 \quad \text{in } \Omega, \qquad (1.25)\\
&\tilde{\mathbf{u}}^m = \mathbf{0} \qquad\qquad \text{on } \partial\Omega. \qquad (1.26)
\end{aligned}$$

On putting $\epsilon = k$ in (1.24)-(1.26), this system may be considered as a semi-implicit temporal discretization of $(\tilde{\beta} \geq 0)$

$$\begin{aligned}
&\mathbf{u}_t^\epsilon - \tilde{\beta}\nabla\operatorname{div}\mathbf{u}_t^\epsilon - \nu\Delta\mathbf{u}^\epsilon + \big(\mathbf{P}_{\mathbf{J}_0}\mathbf{u}^\epsilon\cdot\nabla\big)\mathbf{u}^\epsilon + \nabla p^\epsilon = \mathbf{0} \quad \text{in } \Omega_T, \qquad (1.27)\\
&\operatorname{div}\mathbf{u}^\epsilon + \epsilon p = 0 \quad \text{in } \Omega_T, \qquad (1.28)\\
&\mathbf{u} = \mathbf{0} \qquad\qquad \text{on } \partial\Omega. \qquad (1.29)
\end{aligned}$$

For $\tilde{\beta} = 0$, this formulation is known as penalty method, which is studied in [12], and [7, Section 3.2]. Hence, (1.27) is a modification thereof, which uses the additional term $-\tilde{\beta}\nabla \mathrm{div}\, \mathbf{u}_t^\epsilon$ to additionally enforce the incompressibility constraint for $\tilde{\beta} > 0$.

Another interpretation of system (1.24)-(1.26) for $\beta = 1$ comes from its reformulation

$$d_t \tilde{\mathbf{u}}_k^m - \frac{1}{k}\nabla \mathrm{div}\, \tilde{\mathbf{u}}_k^m - \nu\Delta\tilde{\mathbf{u}}_k^m + \big(\mathbf{P}_{\mathbf{J}_0}\tilde{\mathbf{u}}_k^{m-1}\cdot\nabla\big)\tilde{\mathbf{u}}_k^m = \mathbf{f}^m. \tag{1.30}$$

As a consequence, iterates $\{\tilde{\mathbf{u}}_k^m\}_m \subset \mathbf{H}_0^1(\Omega)$ from Algorithm C solve an implicit temporal discretization of the penalty formulation (1.27)-(1.29), with $\epsilon = k$, and $\tilde{\beta} = 0$ For $\beta \geq 1$, the system combines different stabilizing mechanisms to enforce the incompressibility constraint for iterates $\{\tilde{\mathbf{u}}_k^m\}$. Also, (1.30) is an implicit discretization to effectively describe iterates $\{\tilde{\mathbf{u}}_k^m\}$ in this case, and does not require initial data for the pressure; this is in contrast to Algorithm C, due to the (decoupling) projection step to obtain $\{\mathbf{u}^m\}_m \subset \mathbf{J}_0$.

Note that no unphysical boundary conditions, and no accurate initial data for the pressure are needed in (1.24)-(1.26) any more. The following result is shown in [9] for general strong solutions of (1.1)-(1.4),

$$\max_{1\leq m\leq M}\Big[\|\tilde{\mathbf{u}}^m - \mathbf{u}(t_m,\cdot)\|_{\mathbf{L}^2} + \sqrt{\tau_m}\,\|\tilde{\mathbf{u}}^m - \mathbf{u}(t_m,\cdot)\|_{\mathbf{W}^{1,2}} + \tau_m\,\|p^m - p(t_m,\cdot)\|_{L^2}\Big] \leq C\,k. \tag{1.31}$$

From (1.19) and (1.31), we may conclude that pressure iterates from Algorithms B and C are comparable.

Over the last two decades, many different projection schemes to efficiently solve (1.1)-(1.4) have been constructed and studied, cf. [4]; hence, Algorithms A to C only represent some second- and first-order time-discretizations out of them. However, a numerical analysis of each of these (higher order) projection methods shares the following common challenges:

(i) limited regularity of solutions of (1.1)-(1.4),
(ii) avoidance of requiring accurate initial data for the pressure, which are nontrivial to obtain with sufficient accuracy, and
(iii) smallness or absence of artificial boundary data for the pressure.

This is the authors' motivation for the upper selection of schemes, and presentation of tools to overcome those inherent limitations (i.e., artificial boundary layers, regularity requirements of solutions of (1.1)-(1.4), assumed known initial pressure) of earlier projection schemes.

The remainder of this work is organized as follows: In Section 2, we compare the accuracy of pressure iterates obtained from Algorithms A to C, where the initial pressure is not available explicitly. Conclusions are made in Section 3.

2. Computational Experiments

We computationally compare the accuracy of pressure iterates from the second-order schemes, i.e., Algorithms A (Van Kan scheme) and B (revised Van Kan scheme). As has been pointed out, the original Van Kan scheme suffers from the need to provide accurate initial data, and smoothness of solutions of (1.1)-(1.4), in order to validate (1.10). Algorithm B, together with

the mesh $\mathcal{G}_2(k_m)$ has been designed to introduce an additional damping mechanism into the scheme to reliably overcome the initial time period $[0,1]$.

Another strategy to obtain accurate pressure approximations is realized in Algorithm C (Chorin-Penalty scheme), where Chorin's first-order projection scheme is modified in such a way that formerly arising numerical boundary layers are avoided. The following example for the evolutionary Stokes problem is to compare higher order projection schemes, creating small artificial boundary layers for pressure iterates, with first-order projection methods exempted from this deficiency. The examples are meant to illustrate arising time-layer structures for iterates of Algorithm A for absent nonlinear convection.

Example 2.1 (from [4]) Let $\Omega = (-1,1)^2 \subset \mathbb{R}^2$, and

$$\mathbf{u}(x,y,t) = \begin{pmatrix} \pi \sin\, t\, \sin 2\pi y\, \sin^2 \pi x \\ -\pi \sin\, t\, \sin 2\pi x\, \sin^2 \pi y \end{pmatrix}, \qquad p(x,y,t) = \sin\, t\, \cos \pi x\, \sin \pi y,$$

be solutions of the evolutionary Stokes problem, i.e., $\mathbf{f} : \Omega_T \to \mathbb{R}^2$ is computed from (1.1)-(1.4), where the nonlinear term in (1.1) is neglected. Let $\mathcal{T}_h$ be an equi-distant triangulation of Ω of mesh-size $h = 1/30$, and $k = 2^{-j}/500$, $j = 0,1,2,3$ an equidistant time-step for the time interval $[0,1]$. The LBB-stable MINI-Stokes element is used for spatial discretization of the three projection methods, and $\tilde{p}^0 = p^0 = 0$ is chosen. For the solution of the system of linear equation we used the direct solver.

We computed all the examples with zero initial pressure, which is the correct initial data. In Fig. 2.1, we plot L^2-errors for iterates of Algorithms A to C to compare the behavior of the three algorithms which shows comparative results for the higher order schemes A and B, with slightly improved convergence properties of B; at positive times, the overall error is dominated by spatial discretization effects. Iterates of the first-order scheme C are of non-comparable quality.

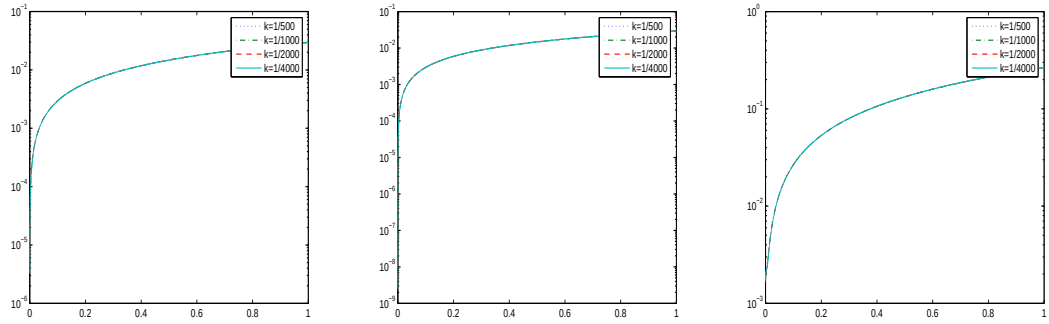

Fig. 2.1. Example 2.1: Evolution of the L^2 norm of the pressure error for the Algorithms A,B and C (left to right)

Since in practical computations the initial pressure is not known, we take another example with a polynomial solution, in order to see the effects of the noncorrect initial data and the difference between first-order and second-order projections.

Example 2.2. Let $\Omega = (0,1)^2 \subset \mathbb{R}^2$, and

$$\mathbf{u}(x,y,t) = \begin{pmatrix} x^2(1-x)^2(2y - 6y^2 + 4y^3) \\ -y^2(1-y)^2(2x - 6x^2 + 4x^3) \end{pmatrix}, \qquad p(x,y,t) = \left(x^2 + y^2 - \frac{2}{3}\right)(1+t^2),$$

be solutions of the evolutionary Stokes problem, i.e., $\mathbf{f} : \Omega_T \to \mathbb{R}^2$ is computed from (1.1)-(1.4), where the nonlinear term in (1.1) is neglected. Let $\mathcal{T}_h$ be an equi-distant triangulation of Ω of mesh-size $h = 1/30$, and $k = 2^{-j}/500$, $j = 0, 1, 2, 3$ an equidistant time-step for the time interval $[0, 1]$. The LBB-stable MINI-Stokes element is used for spatial discretization of the three projection methods, and $\tilde{p}^0 = p^0 = 0$ is chosen. For the solution of the system of linear equation we used the direct solver.

Plots of evolving L^2-errors for iterates of Algorithms A to C (with $\beta = 1.1$) at times $t = 0.05, 0.1, 0.3, 1$ are shown in Fig. 2.4. We observe marked errors only for Algorithm A at times close to zero, as opposed to uniform small errors in space-time for Algorithms B, C. In Fig. 2.3, we plot L^2-errors for iterates of Algorithms A to C to compare the behavior of the three algorithms. We remark that the given m-dependent coefficients in Algorithm B which uses $\mathcal{G}_2(k_m)$ are essential to implement, and otherwise lead to divergent results.

Plots of evolving L^2-errors for iterates of Algorithms A to C are shown in Fig. 2.2. We observe marked layers in time for pressure iterates in the case of Algorithm A, as opposed to iterates from Algorithms B and C. The depicted oscillatory behavior in the error plot vanishes for

$$m \mapsto \|p(t_m, \cdot) - p^{m-1/2}\|_{L^2},$$

see also (1.10) and (1.19).

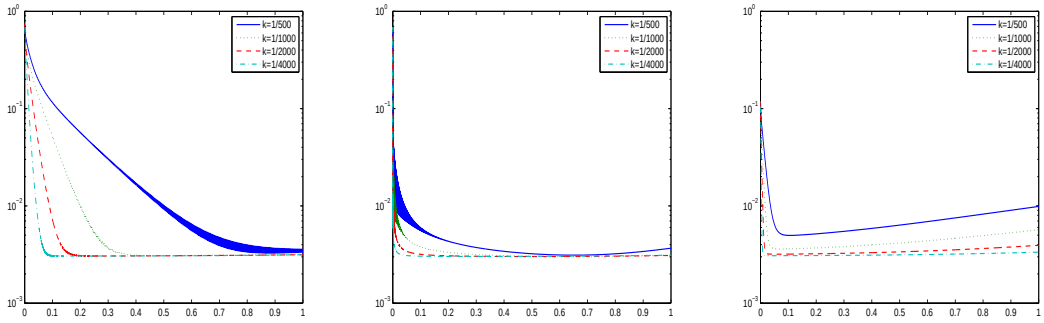

Fig. 2.2. Example 2.2: Evolution of the L^2 norm of the pressure error for the Algorithms A,B and C (left to right)

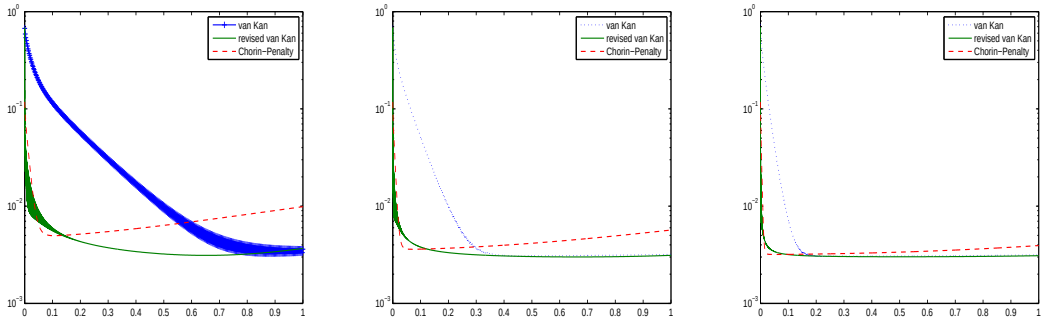

Fig. 2.3. Example 2.2: Comparison of the evolution of the L^2 norm of the pressure error for the Algorithms A,B and C for $k = 1/500, 1/1000, 1/2000$ (left to right)

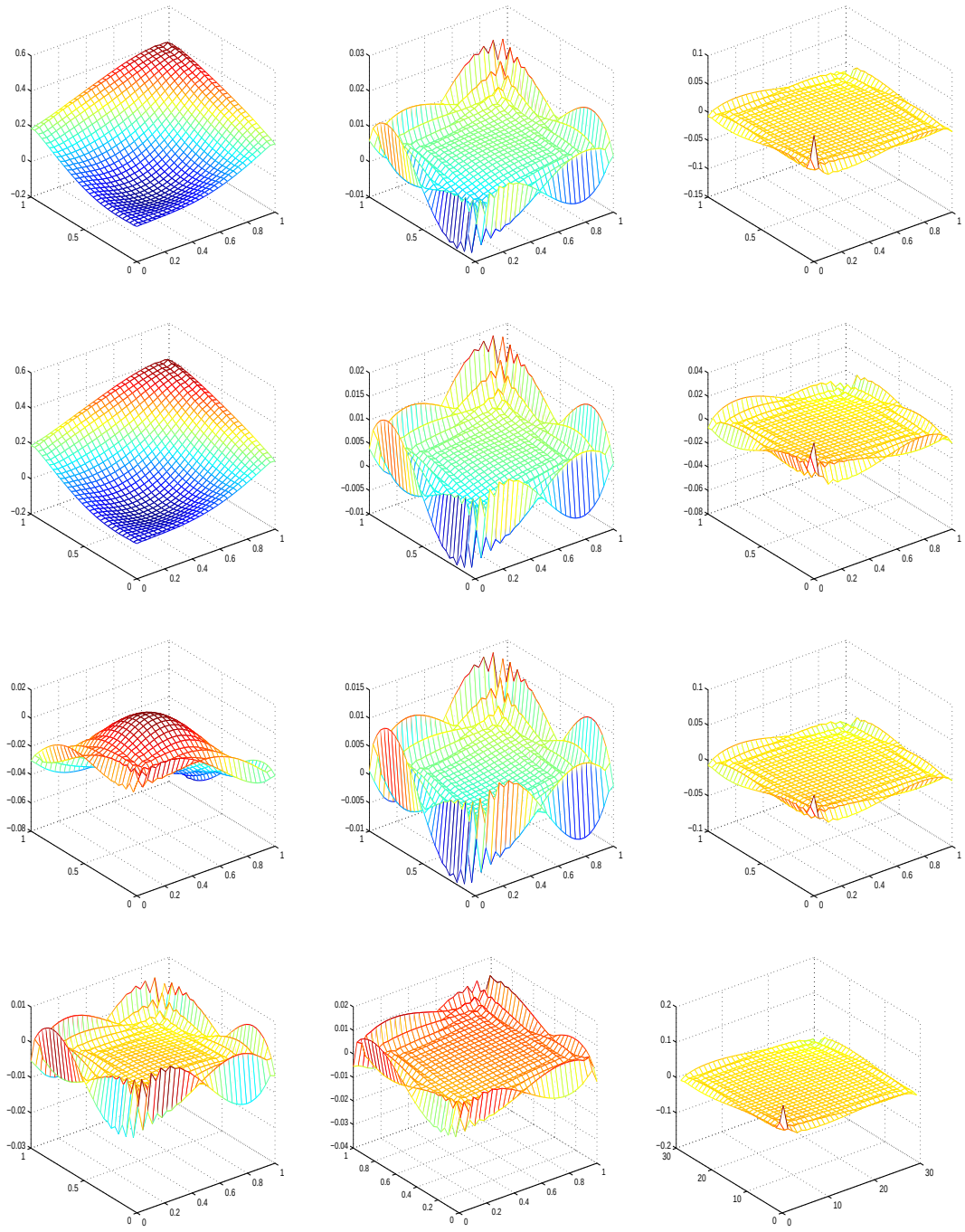

Fig. 2.4. Example 2.2: Snapshots of the pressure error at time $T = 0.05, 0.1, 0.3, 1$ (top to bottom) for $k = 1/500$ for the Algorithms A,B and C (left to right)

3. Concluding Remarks

Projection methods are efficient methods to approximate strong solutions of the nonstationary incompressible Navier-Stokes equations; the most well-known example is Chorin's method,

which suffers from marked pressure error boundary layers. There are two strategies available to cure this deficiency: either (i) modify this scheme in such a sense that the mechanism responsible for boundary layers is eliminated, i.e., Algorithm C (Chorin-Penalty method), or (ii) use a higher order projection method where this effect is significantly reduced (Van Kan scheme). The second approach, however, has to face other critical issues in the construction process, which are the expected breakdown of the regularity of solutions to (1.1)-(1.4), and, typically, the need of accurate initial data for such schemes. Algorithm B (revised Van Kan scheme) uses a stretched time-grid structure $\mathcal{G}_2(k_m)$, and is designed to overcome both of these hurdles: the error estimate (1.19) for corresponding iterates is comparable to the one of the fully implicit Crank-Nicholson method (see, e.g.(1.5)), while the scheme keeps all advantages of a (higher-order) projection scheme. The comparative computational studies shown above illustrate these considerations.

Acknowledgment. This is an extended version of a talk presented during the Second Chinese-German Workshop on Computational and Applied Mathematics in Hangzhou (October 9-13, 2007).

References

[1] A.J. Chorin, Numerical solution of the Navier-Stokes equations, *Math. Comput.*, **22** (1968), 745-762.

[2] A.J. Chorin, On the convergence of discrete approximations of the Navier-Stokes equations, *Math. Comput.*, **23** (1969), 341-353.

[3] W.E, J.G. Liu, Projection method I: Convergence and numerical boundary layers, *SIAM J. Num. Anal.*, **32** (1995), 1017-1057.

[4] J.L. Guermond, P. Minev, J. Shen, An overview of projection methods for incompressible flows, *Comput. Method. Appl. M.*, **195** (2006), 6011-6045.

[5] J.G. Heywood, R. Rannacher, Finite element approximation of the nonstationary Navier-Stokes problem. I. Regularity of solutions and second-order error estimates for statial discretization, *SIAM J. Numer. Anal.*, **19** (1982) 275-311.

[6] J.G. Heywood, R. Rannacher, Finite element approximation of the nonstationary Navier-Stokes problem. IV. Error analysis for second-order time discretization, *SIAM J. Numer. Anal.*, **27** (1990), 353-384.

[7] A. Prohl, Projection and Quasi-Compressibility Methods for Solving the Incompressible Navier-Stokes Equations, Teubner-Verlag, Stuttgart, 1997.

[8] A. Prohl, A first-order projection-based time-splitting scheme for computing chemically reacting flows, *Numer. Math.*, **84** (2000), 649-477.

[9] A. Prohl, On pressure approximation via projection methods for nonstationary incompressible Navier-Stokes equations, *SIAM J. Numer. Anal.*, (accepted, 2008).

[10] R. Rannacher, On Chorin's projection method for the incompressible Navier-Stokes equations, in: *LNM* **1530**, eds.: J.G. Heywood, K. Masuda, R. Rautmann, S.A. Solonnikov: The Navier-Stokes Equations II – Theory and Numerical Methods, Proc. Oberwolfach (1991), 167-183.

[11] J. Shen, On error estimates of projection methods for the Navier-Stokes equations: Second-order schemes, *Math. Comput.*, **65** (1996), 1039-1065.

[12] J. Shen, On error estimates of the penalty method for unsteady Navier-Stokes equations, *SIAM J. Numer. Anal.*, **32** (1995), 386-403.

[13] R. Temam, Sur l'approximation de la solution des equations de Navier-Stokes par la methode des pas fractionnaires II, *Arch. Ration. Mech. An.*, **33** (1969), 377-385.

[14] Van Kan, A second-order accurate pressure-correction scheme for viscous incompressible flow, *SIAM J. Sci. Stat. Comput.*, **7** (1986), 870-891.